FERMILAB-PUB-12-280-E

Final State Interactions Effects in Neutrino-Nucleus Interactions

Tomasz Golan* and Cezary Juszczak
Institute for Theoretical Physics, Wrocław University
Plac Maxa Borna 9, 50-204 Wrocław, Poland

Jan T. Sobczyk
Fermi National Accelerator Laboratory, Batavia, Illinois 60510, USA†

Final State Interactions effects are discussed in the context of Monte Carlo simulations of neutrino-nucleus interactions. A role of Formation Time is explained and several models describing this effect are compared. Various observables which are sensitive to FSI effects are reviewed including pion-nucleus interaction and hadron yields in backward hemisphere. NuWro Monte Carlo neutrino event generator is described and its ability to understand neutral current π^0 production data in ~ 1 GeV neutrino flux experiments is demonstrated.

I. INTRODUCTION

New generation of neutrino oscillation parameters measurements require a good knowledge of neutrino-nucleus cross sections. Experimental data analysis is always based on predictions from Monte Carlo (MC) event generators [1]. In the 1 GeV energy region, characteristic for several oscillation experiments (MINOS, T2K, MiniBooNE, NOvA) the use of the Impulse Approximation (IA) picture [2] in which neutrinos scatter on individual quasi-free nucleons is well justified. In this picture any neutrino-nucleus interaction is a two-step process: (i) the primary scattering on a bound nucleon, and (ii) Final State Interactions (FSI) affecting the hadrons produced at the step (i). The FSI contribute significantly to the systematic errors in neutrino oscillation measurements so it is important to develop models to describe them better and also to understand the models' limitations [3].

MC codes used in major neutrino oscillation experiments (FLUKA [4], NUANCE [5], NEUT [6], GENIE [7]) in their description of FSI effects rely on the model of intra-nuclear cascade (INC) [8]. It is a semi-classical approach in which some quantum effects can also be incorporated (Pauli blocking, formation time (FT), nucleon correlations). Theoretical arguments for the applicability of the cascade model go back to the works of Glauber [9]. More recently the investigation of the cascade model in the Δ resonance region was done in [10]. The model predictions agree with the experimental data for the pion-nucleus reaction cross sections, including the pion absorption.

While the basic idea behind the models of FSI in the MC codes is always the same, numerical implementations are quite different reflecting priorities of particular neutrino experiments (target, detection technique etc).

An important and not sufficiently understood ingredient in the INC models are the Formation Time (FT) effects. On the most fundamental level the FT is related to the Quantum Chromodynamics phenomenon called the color transparency (CT), proposed by Brodsky and Mueller [11]. For high enough four-momentum transfers a quark system is created with a small transverse size (Point-Like Configuration - PLC) which is supposed to suppress hadrons re-interactions. As the typical size of the PLC is of the order of $1/|Q|$ [12], the CT effects are expected to be seen mostly at higher energies. Moreover, two-quark systems are more likely to create PLC than three-quark ones so the effect is expected to be larger for pions, than for nucleons.

Independent phenomenological considerations [13], [14] led to the construction of approximate models of FT. As will be shown in Sect IV many evaluations of basic parameters which determine the size of FT effects have been proposed. It seems important to study them explicitly in the context of neutrino measurements. For example, the FT effects are in the obvious interplay with the pion absorption, reducing its probability in a non trivial momentum dependent way.

Validation of FSI models can be done using any hadronic observables as all of them are FSI sensitive. Such observables include: distributions of numbers of reconstructed hadron tracks, spectra of hadrons in the final state, their angular distributions etc. FSI models used in neutrino MC simulations can also be validated on electro- and photo- nucleus observables. In the analysis of the NOMAD high energy neutrino scattering data [15] the introduction of the FT was necessary to get agreement between one and two track quasielastic samples of events. It is interesting that the analysis of hadron-nucleus scattering data within INC models indicates that also at lower energies the FT effects can be important [16].

In this paper FSI effects are modeled within the NuWro MC event generator [17]. NuWro covers neutrino energy range from a few hundreds MeV (the limit of applicability of the Impulse Approximation) to several TeV. The code has flexibility to include Spectral Function [18] formalism with sophisticated nuclear effects, as an alternative to the Fermi Gas model or a momentum dependent effec-

* tgolan@ift.uni.wroc.pl
† On leave from the Institute for Theoretical Physics, Wrocław University

Operated by Fermi Research Alliance, LLC under Contract No. De-AC02-07CH11359 with the United States Department of Energy.

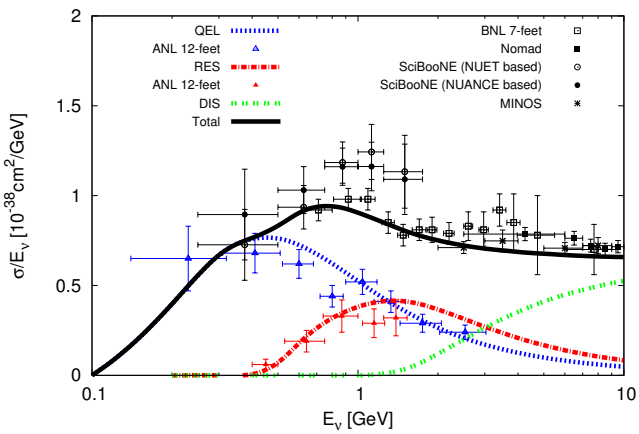

FIG. 1. (Color online) NuWro predictions for CC scattering cross section (per nucleon) on free isoscalar target in QEL, RES and DIS channels. The data points are taken from: ANL 12-feet (QEL) [21], ANL 12-feet (RES) [22], BNL 7-feet [23], Nomad [24], SciBooNE [25], MINOS [26].

tive potential [19]. NuWro allows for comparisons to the data reported by experimental groups in the FSI effects included format.

We will consider a model of FT which is validated on the NOMAD backward moving pions data. We will then discuss the NC π^0 production and see how important the FT effects are for the understanding of the experimental data. The NC $1\pi^0$ production is a very important process because it is a background to the $\nu_\mu \to \nu_e$ oscillation search in water Cherenkov detectors: it can happen that one of the two photons from the π^0 decay remains undetected and the other is reconstructed as an electron. The NC $1\pi^0$ production is also a very useful reaction to validate FSI models in the 1 GeV energy region. It is very sensitive to pion absorption and it is important to investigate the relevance of the FT effects which make the nuclear environment more transparent for pions produced inside nucleus.

The paper is organized in the following way. In Sect. 2 a general description of the NuWro MC model is given. In Sect. 3 the NuWro FSI model based on the theoretical approach of Oset [10] is described. Several tests are reported showing a good agreement with the original numerical implementation. Sect. 4 contains a summary of various ways to model the FT. Various approaches considered in the context of neutrino interactions and parameters used in theoretical computations and in MC codes are discussed. In Sect 5 the NuWro predictions are compared with the NC $1\pi^0$ production data and the significance of the FT effects is discussed. Our conclusions are contained in Sect 6.

II. NUWRO

NuWro [17] is a neutrino event generation software developed at the Wrocław University. The main motivation for the NuWro authors was to have a tool to investigate the impact of nuclear effects on directly observable quantities, with all the FSI effects included. Since 2005 it evolved into a fairly complete neutrino interactions modeling tool. Its basic architecture is similar to better known MCs like NEUT or GENIE. All major neutrino-nucleus interaction channels are implemented and the commonly used relativistic Fermi Gas (FG) model is for certain nuclei replaced with the more realistic Spectral Function model [18]. The NuWro FSI code has recently been updated by incorporating the Oset model [10] of effective pion-nucleon cross sections and several options for the FT. Other upgrades include: parameterization of the multipion production cross section in pion-nucleon collisions based on the available data and the implementation of angular distributions in elastic and charge exchange pion-nucleon scattering based on the SAID model [20].

With the inclusion of realistic beam models and a detector geometry module NuWro is becoming a fully-fledged MC event generator ready for use in neutrino experiments.

A. Interactions

In NuWro there are four basic dynamic channels: quasi-elastic (QEL), resonance (RES), more inelastic (DIS) and coherent pion production (COH), each can be either in the charged current (CC) or in the neutral current (NC) mode. The eight channel/mode combinations can be individually enabled or disabled. The code is quite effective and all the cross sections are calculated in the real time. The typical simulation output consists of a table of average cross sections (per nucleon) for all the dynamical channels and a sample of equal weight events of the chosen size. In Fig. 1 NuWro predictions for cross sections on isoscalar target from various dynamical channels are shown. In the CCQE channel the axial mass was chosen to be $M_A = 1030$ MeV. The SciBooNE inclusive CC cross section measurement done on the carbon taget can contain a large Meson Exchange Current contribution which is not present in the NuWro simulations. This can explain why at $E_\nu \sim 1$ GeV SciBooNE data points are above the NuWro predictions.

For each (but the coherent) channel a particular nucleon which will take part in the interactions is picked up with nuclear matter density used as the probability density. Its momentum is chosen from a ball with the radius set to the Fermi momentum (or the local Fermi momentum calculated for that density in the case of LDA) or obtained as a draw from the Spectral Function.

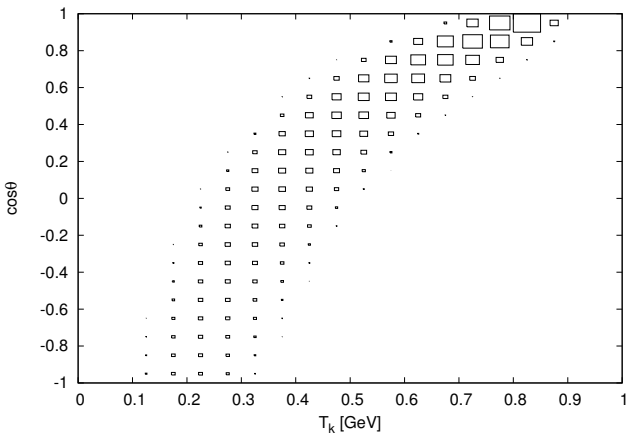

FIG. 2. Double differential cross section in muon scattering angle and kinetic energy for 1 GeV CCQE muon neutrino interaction with carbon as predicted by NuWro FG model implementation. The boxes areas are proportional to the cross section. The maximal cross section is $7.28 \cdot 10^{-41} cm^2/GeV$.

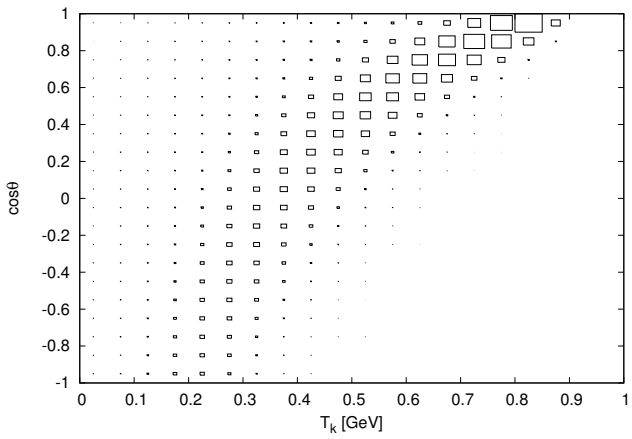

FIG. 3. Same as Fig. 2, but Fermi Gas is replaced by the Spectral Function The maximal cross section is $5.77 \cdot 10^{-41} cm^2/GeV$.

1. QEL

The CC quasi-elastic and NC elastic reactions are handled by the QEL channel. It uses the standard Llewellyn Smith formulae [27] with several options for the vector form factors (dipole, BBA03 [28], BBBA05 [29], Alberico et al [30]).

The global and local relativistic FG models or the SF approach are typically used but the kinematics based on the momentum dependent nuclear potential [19] is also available. Currenly, the Spectral Functions for carbon, oxygen, argon, calcium and iron are implemented in NuWro with the tables obtained from Omar Benhar or as calculated in [31]. In the SF mode the de Forest kinematical prescription [32] is used.

Figs 2–3 shows NuWro predictions for 1 GeV muon neutrino CCQE scattering on carbon calculated with Fermi Gas and Spectral Function models. The shapes of 2D differential cross sections are similar. In the case of FG the cross section is larger by $\sim 10\%$. SF allows for much larger phase space for the final state muons.

2. RES

The RES channel is defined as $W < 1.6$ GeV, where W is the invariant hadronic mass. The dominant contribution comes from single pion production mediated by the $\Delta(1232)$ resonance. All possible channels are implemented. Axial form-factors are taken from the reanalysis of the ANL and BNL bubble chambers data [33]. Not using the standard Rein-Sehgal model [34] of resonance production to describe the contribution from higher resonances is justified by the quark-hadron duality hypothesis [35] and by the fact that higher resonances cannot be separated in lepton-nucleus scattering. The non-resonant background is modeled as a fraction of the DIS contribution for $W \in (1.3, 1.6)$ GeV scaled so as the passage to the pure DIS channel be smooth. The RES channel includes also a small two pion production component which is evaluated using the same prescription as used for the DIS channel.

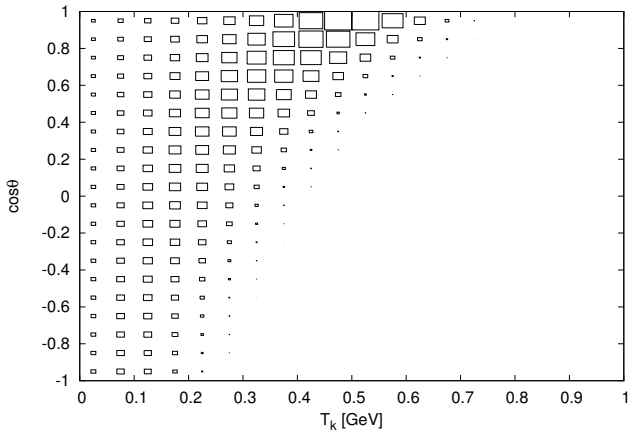

FIG. 4. Same as Fig. 2, but for the RES channel. The maximal cross section is $1.40 \cdot 10^{-41} cm^2/GeV$.

Fig. 4 shows NuWro predictions for 1 GeV muon neutrino RES scattering on carbon.

3. DIS

The DIS channel is defined as $W > 1.6$ GeV. The total cross sections are evaluated using the Bodek-Yang

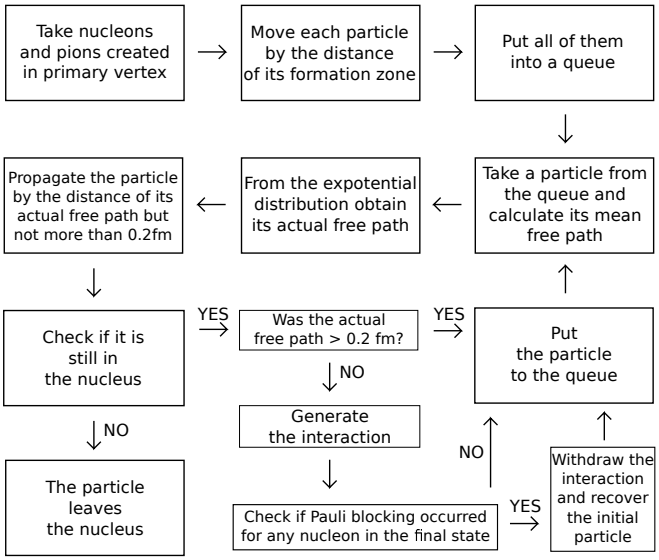

FIG. 5. A block diagram of the NuWro INC algorithm.

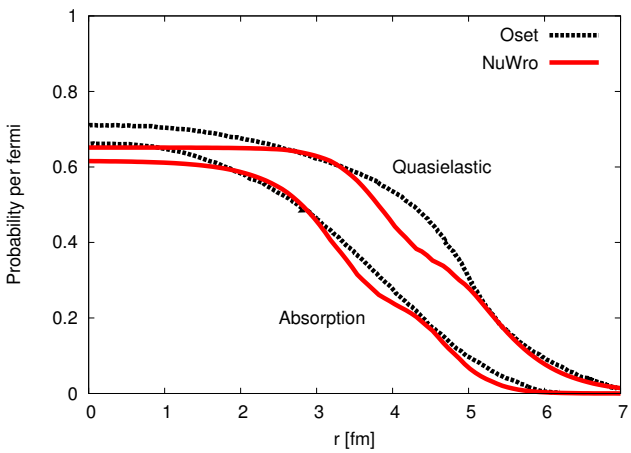

FIG. 6. (Color online) Probability (per fermi) of microscopic pion-nucleon interactions in Iron as a function of distance from the nucleus centre. Pion kinetic energy $T_k = 165$ MeV. The Oset model results are taken from [10].

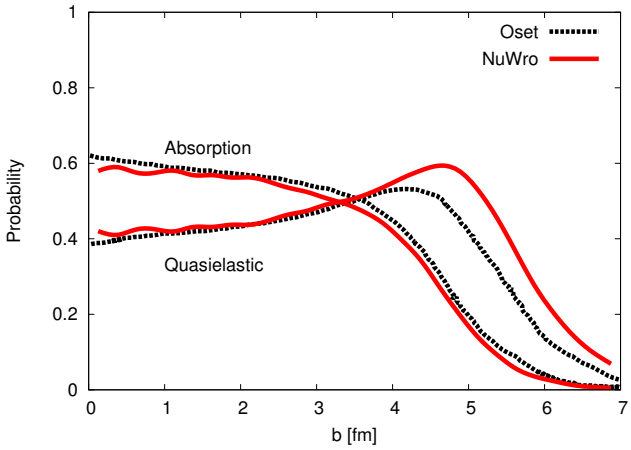

FIG. 7. (Color online) Probability of macroscopic quasi-elastic or absorption interactions as a function of an impact parameter b for π^+ ^{40}Ca scattering with pion kinetic energy $T_k = 180$ MeV. The Oset model results are taken from [10].

prescription [36]. The Pythia6 hadronization routine is called for specific quark configurations [37] to allow their meaningful use also in the small W region down to 1.2 GeV used in modelling the background for RES. The performance of the hadronization model was checked by comparing to the available hadron production multiplicities data [38].

4. COH

The coherent pion production is implemented using the Rein-Sehgal model [39] with lepton mass corrections.

III. NUWRO FSI MODEL

The NuWro FSI effects are described in the framework of the INC model [8]. The neutrino interaction point is selected inside the nucleus according to the nuclear matter density. All secondary hadrons propagate through the nucleus and can interact with nucleons inside. In the code the 0.2 fm step length is assumed. To be more specific, the reinteraction can happen at any point of the path, but the nuclear density is probed in intervals not exceeding 0.2 fm. For smaller values of the step the results remain the same, only running time increases. Between the collisions hadrons are assumed to be on-shell and move in straight lines. The actual free path is a draw from the exponential distribution calculated based on an effective cross section model. The generic re-interaction algorithm is independent on the dynamics used, also different models of nuclear density can be used. The particular dynamics is taken from the Oset model [10] and has solid theoretical foundations. The model is supposed to work well in the most important Δ region for pion kinetic energies in the range $85 - 350$ MeV. Outside this region the cross sections are obtained from the available pion-nucleon scattering data.

The basic FSI scheme, see Fig. III, consists in putting nucleons and pions produced in the primary and also in secondary interactions to a queue and repeating the following until the queue gets empty:

(a) take a particle from the queue,

(b) examine the nucleus density at its position,

(c) calculate the mean free path,

(d) probe the exponential distribution for the actual free path,

(e) if the selected path is bigger then 0.2 fm adjust the particle position by 0.2 fm,

- if the particle is still in the nucleus put it at the end of the queue,
- if the particle is outside the nucleus put it to the list of outgoing particles,

  1° nucleons kinetic energy is diminished by the value of the potential:

  $$V = \sqrt{M^2 + k_f^2} - M + 8\ MeV$$

  where k_f is the Fermi momentum and its momentum is adjusted so that it remains on shell.

  2° if nucleons kinetic energy is smaller then V the step 1° cannot be completed. The nucleon is assumed to be unable to leave nucleus. It is reinserted to the nuclear matter and its kinetic energy contributes to the nucleus excitation energy,

(f) if the selected path is smaller that 0.2 fm assume that interaction with nuclear matter happened at this very place,

(g) probe the target nucleon momentum from the Fermi ball with the local Fermi momentum calculated from the density at that point,

(h) select the type of interaction and generate the kinematics,

(i) check if none of the resulting nucleons is Pauli blocked; in the case of Pauli blocking forget the interaction, reinsert particle to the queue at the failed interaction point (Pauli blocking effects can be also included by means of increased values of the mean free paths and then this step of the algorithm must be skipped),

(j) if the interaction was not Pauli blocked, all the particles in the final state are put to the end of the queue.

(k) if FT/FZ effects apply also to secondary interactions (this is model dependent) the particles positions are accordingly adjusted.

The nucleus radius is defined as a distance from the center, where the density is smaller by a factor of 10^4 than the maximal one.

As a result of some nucleons joining the INC, the nuclear matter density is reduced but the shape of the density profile is assumed to be unchanged.

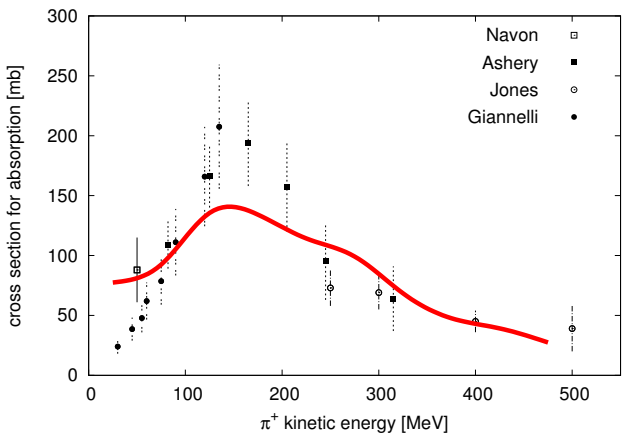

FIG. 8. (Color online) The π^+ ^{12}C absorption cross section. The data points are taken from: Ashery [41], Navon [42], Jones [43] and Giannelli [44]. The solid line shows NuWro predictions.

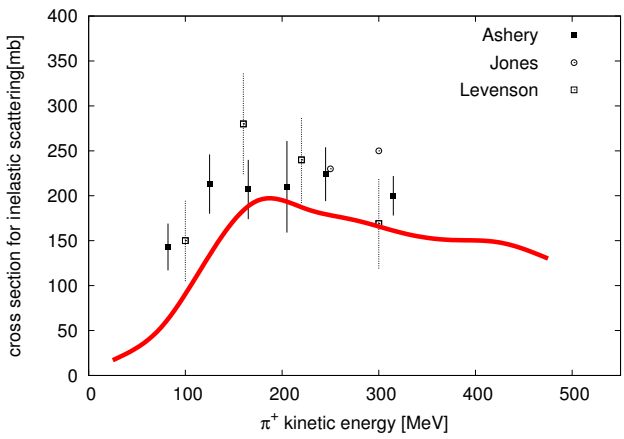

FIG. 9. (Color online) The π^+ ^{12}C inelastic cross section. The data points are taken from: Ashery [41], Jones [43], and Levenson [45]. The solid line shows NuWro predictions.

A. The Oset model

On the microscopic level the Oset model includes the quasi-elastic pion-nucleon reaction (with the charge exchange channel) and the pion absorption with two- and three-body absorption mechanisms. The interaction probability per time unit is:

$$Pdt = -\frac{1}{\omega}\,\mathrm{Im}(\Pi)dt = -2\,\mathrm{Im}(V_{opt})dt \qquad (1)$$

where ω is the pion energy, Π is the pion self-energy, and V_{opt} is the optical potential.

In the simplest case of $\pi^+p \to \pi^+p$ p-wave scattering

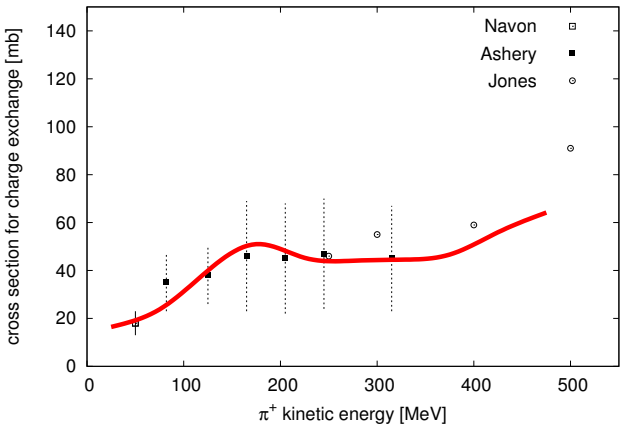

FIG. 10. (Color online) The π^+ ^{12}C charge exchange cross section. The data points are taken from: Ashery [41], Navon [42], and Jones [43]. The solid line shows NuWro predictions.

calculations lead to the result:

$$P = \frac{1}{\omega}\frac{2}{3}\left(\frac{f^*}{m_\pi}\right)^2 q_{c.m.}^2 |G_\Delta(q)|^2 \frac{1}{2}\Gamma\rho_p \tag{2}$$

where f^* is $\pi N\Delta$ coupling constant $\left(f^{*2}/4\pi = 0.36\right)$, m_π is the pion mass, $q_{c.m.}$ is the pion momentum in the centre of mass system, G_Δ is Δ propagator, Γ its width and ρ_p is the proton density.

An important in-medium effect is the Δ self-energy. Its imaginary part can be parameterized as [40]:

$$\mathrm{Im}\,\Sigma_\Delta(\omega) = -\left[C_Q(\rho/\rho_0)^\alpha + C_{A2}(\rho/\rho_0)^\beta + C_{A3}(\rho/\rho_0)^\gamma\right] \tag{3}$$

The Δ width is modified $\frac{1}{2}\tilde{\Gamma} \to \frac{1}{2}\tilde{\Gamma} - \mathrm{Im}\,\Sigma_\Delta$, changing the Δ propagator and producing extra terms in Eq. (2), proportional to functions C's present in Eq.(3). The term proportional to C_Q corresponds to higher order quasi-elastic scattering and the terms with C_{A2} and C_{A3} correspond to two- and three-body absorption. ρ is the nuclear matter density and $\rho_0 = 0.17 fm^{-3}$ is the normal density.

The final expression for the interaction probability in the nuclear matter is:

$$P = \frac{1}{\omega}\int \frac{d^3k}{(2\pi)^3} n(\vec{k}) \frac{2}{3}\left(\frac{f^*}{m_\pi}\right)^2 q_{c.m.}^2 |G_\Delta(q+k)|^2 \frac{1}{2}\tilde{\Gamma}(q+k) \tag{4}$$

where $n(\vec{k})$ is the occupation number for protons/neutrons.

The Δ self-energy depends strongly on the nuclear density and the pion absorption is more likely to occur in the central part of the nucleus.

Finally, there are improvements to the model coming from: πN interaction s-wave contribution, the real part of the optical potential and finite size effects.

	T_π = 85 MeV			T_π = 245 MeV			
	n=1	n=2	n=3	n=1	n=2	n=3	n=4
Oset	0.90	0.09	0.01	0.69	0.25	0.05	0.01
NuWro	0.89	0.10	0.01	0.67	0.24	0.07	0.02

TABLE I. Probabilities that macroscopic quasi-elastic process proceeds through n microscopic collisions. Oset model results are taken from [10].

	T_π = 85 MeV			T_π = 245 MeV			
	n=0	n=1	n=2	n=0	n=1	n=2	n=3
Oset	0.81	0.17	0.02	0.37	0.41	0.17	0.04
NuWro	0.87	0.12	0.01	0.41	0.37	0.16	0.05

TABLE II. Probabilities that pion absorption occurs after n quasi-elastic microscopic scatterings. Oset model results are taken from [10].

B. NuWro implementation of the Oset model

The Oset model is implemented in NuWro by means of tables containing the cross-sections as functions of the pion kinetic energy at various nuclear matter densities. Because the finite size effects are not universal it was necessary to prepare tables for each isotope separately.

In the analysis of the performance of the cascade model one should distinguish microscopic (pion-nucleon) and macroscopic (pion-nucleus) reactions. Figs 6–7 show a comparison between NuWro implementation and the original Oset model. Fig. 6 shows the inverse of mean free paths (or equivalently: interaction probabilities per fermi) for two microscopic interactions as functions of the distance from the nucleus center. In both cases contributions from pion-proton and pion-neutron reactions are added. There is a significant dependence on the nuclear density: in the central region of the nucleus the absorption probability is large, but in the peripheral region the quasi-elastic scattering dominates overwhelmingly. Fig. 7 shows probabilities of macroscopic processes as functions of the impact parameter. One can see that for small values of the impact parameter the absorption is more likely than the quasi-elastic scattering. One should remember that the incident pion can be absorbed also after one or more microscopic quasi-elastic scatterings.

Tables I–II help to understand other aspects of the π^+ ^{12}C scattering. Again, results from the original Oset paper are compared to the NuWro implementation. Table I presents the probabilities that a macroscopic quasi-elastic event proceeds through n collisions. Table II contains the probabilities that absorption occurs after exactly n microscopic quasi-elastic pion scatterings. The results are shown for two values of incident pion kinetic energy: 85 and 245 MeV. More energetic pions are likely to undergo several scatterings in which they loose a fraction of their energy until they fall into the absorption

peak in the Δ region.

With a satisfactory agreement for microscopic ingredients of the Oset model, we present a comparison of the NuWro cascade model predictions with experimental data for the π^+ ^{12}C scattering (Figs 8 – 10).

One can distinguish the following macroscopic pion-nucleus reactions: elastic, charge exchange, absorption, and inelastic scattering. The results for the double charge exchange reaction are not shown because the cross section is very small. For larger energies the inelastic cross section contains a pion production component.

The cross section measurement of the charge exchange and absorption processes is straightforward. The inelastic cross section is obtained in the indirect way as:

$$\sigma_{inel} = \sigma_{total} - \sigma_{elastic} - (\sigma_{absorption} + \sigma_{CEX}), \quad (5)$$

with the elastic pion-nucleus cross section contribution evaluated based on theoretical and experimental arguments (for details see [41]).

The NuWro predictions are obtained in the standard way by arranging a homogeneous flux of pions and counting the particles in the final state assuming that at least one microscopic interaction took place. In the simulations on carbon the impact parameter is limited to $b < 6.5$ fm. We checked that with larger b values the evaluated cross sections do not change. In the MC simulations one cannot model the elastic pion-nucleus reaction. The sum over all possible interaction channels gives the pion-nucleus reaction cross section.

Figs 8–10 show that the NuWro predictions are in a reasonable agreement with the data. In the near future results from a dedicated experiment measuring pion-nuclei cross sections with the accuracy of 10% will be known [46]. The results will help to upgrade the parameters of the microscopic model used in the NuWro intranuclear cascade.

The FT effects can be also used in the secondary interaction but their impact on the final results is very small.

IV. FORMATION TIME/ZONE

A. Generalities

The concept of Formation Time/Formation Zone (FT/FZ) was introduced by Landau and Pomeranchuk [47] in the context of multiple scattering of electrons passing through a layer of material. In the LAB frame the FT is given as:

$$t = \frac{E}{k \cdot p} \quad (6)$$

where $p^\mu = (E, \vec{p})$ and $k^\mu = (\omega, \vec{k})$ are four-momenta of the electron and the emitted photon respectively. t has the interpretation of the minimal time necessary for a photon to be created.

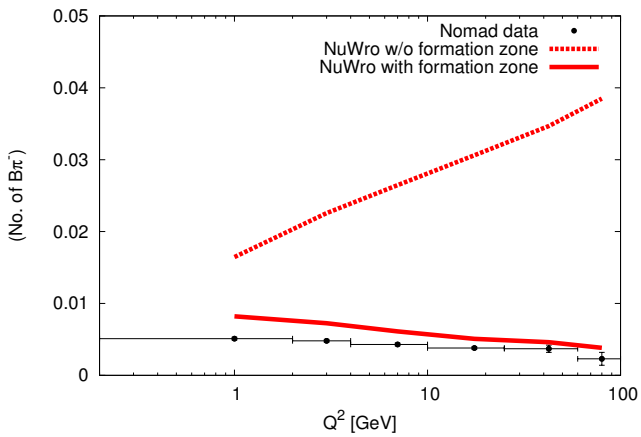

FIG. 11. (Color online) Average number of backward going pions as a function of Q^2 in the NOMAD experiment and in the NuWro simulations.

The idea of FT was applied to hadron production by Stodolsky [13], who considered the production of mesons by protons passing through a nucleus. In the Eq. 6 he replaced the electron by a projectile hadron with a four-momentum $p_0^\mu = (E_0, 0, 0, \sqrt{E_0^2 - M_0^2})$ and the photon by a secondary hadron with a four-momentum $p^\mu = (E, \vec{p}_T, \sqrt{E^2 - p_T^2 - M^2})$ obtaining:

$$t \to t_f = \frac{E_0}{EE_0 - \sqrt{E^2 - p_T^2 - M^2}\sqrt{E_0^2 - M_0^2}} = \frac{1}{E\left(1 - \sqrt{1 - \frac{\mu_T^2}{E^2}}\sqrt{1 - \frac{M_0^2}{E_0^2}}\right)} \quad (7)$$

where μ_T is the transverse mass defined as $\mu_T^2 \equiv M^2 + p_T^2$.

For higher energies $E \gg \mu_T$, $E_0 \gg M_0$ and

$$t_f \approx \frac{2E}{(M_0 x)^2 + \mu_T^2} \quad (8)$$

where $x = \frac{E_0}{E}$. Rantf [14] argued that a further simplification $x \approx 0$ is usually well justified and finally in the LAB frame:

$$t_f \approx \frac{2E}{M^2 + p_T^2} \quad (9)$$

and in the hadron rest frame:

$$t_{f,rest} \approx \frac{2M}{M^2 + p_T^2}. \quad (10)$$

Inspired by this expression Rantf postulated another formula for the FT in the hadron rest frame. He kept the basic relativistic character of the FT but introduced an arbitrary parameter τ_0 to control its size:

$$\tau_{rest} = \tau_0 \frac{M^2}{M^2 + p_T^2}. \quad (11)$$

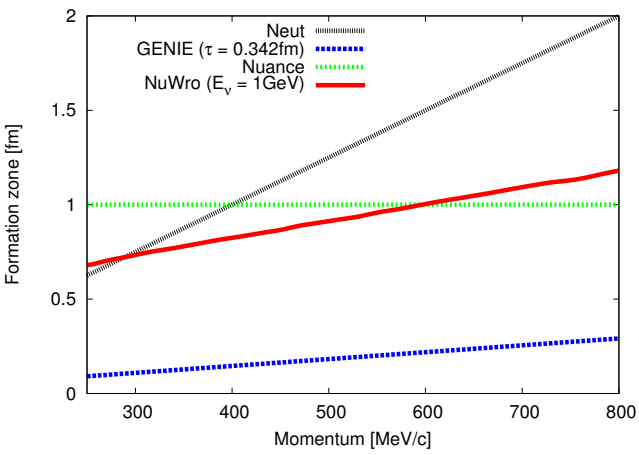

FIG. 12. (Color online) LAB frame nucleon Formation Zone as a function of nucleon momentum.

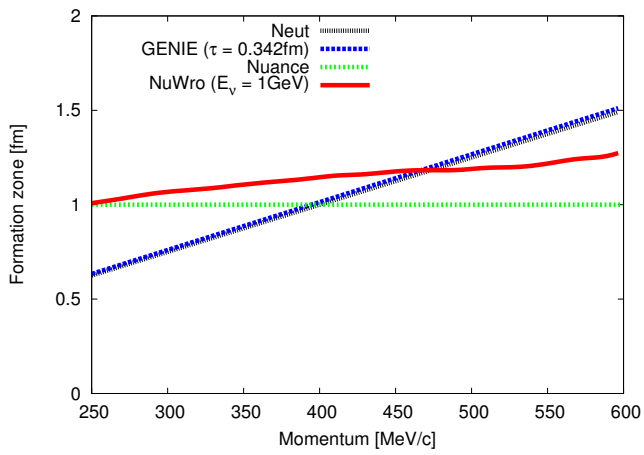

FIG. 13. (Color online) LAB frame pion Formation Zone as a function of pion momentum.

The FT defined in Eq. 11 was implemented in the MC event generator DPMJET [48] which later became a part of the FLUKA code and was used by the NOMAD collaboration [49]. In the DPMJET cascade model the FT is applied to hadrons resulting from all the interaction modes: QEL, RES and DIS. Following the ideas of Bialas [50] the values of FT are sampled from the exponential distribution.

FT played an important role in the NOMAD analysis of the CCQE events [15]. They populate mainly one- and two- tracks samples. A change of τ_0 modifies the MC predictions for the size of both samples: an increase of FT makes an impact of the FSI effects on the ejected protons smaller and they are more likely to have larger momentum with increased probability of being detected and populating the two-track sample of events. By adjusting the size of the formation time the values of M_A calculated independently from either of the two samples of events became almost identical.

In the above estimations of the FT effect several assumptions were made which are not necessarily valid at lower energies. This is taken into account in the more recent low energy FLUKA cascade model, called PEANUT [51]. For QEL reactions FT was replaced by the concept of coherence length (CL).

Derivation of the CL is based on the uncertainty principle arguments: Let p^μ be the outgoing nucleon four-momentum and $q^\mu = (\omega, \vec{q})$ the four-momentum transfer, both in the LAB frame. Because $p \cdot q$ is a Lorentz scalar, one can calculate $\tilde{\omega}$ ($\tilde{}$ refers to quantities calculated in the nucleon rest frame), the energy transfer in the final nucleon rest frame:

$$|p \cdot q| = |\tilde{p} \cdot \tilde{q}| = |\tilde{\omega} M| \Rightarrow |\tilde{\omega}| = \frac{|p \cdot q|}{M} \tag{12}$$

From the uncertainty principle $\tilde{\omega}$ can be used to estimate the reaction time in the nucleon's rest frame and then in the LAB frame. Within that time the nucleon is assumed to be unable to re-interact [52]:

$$t_{CL,rest} = \frac{M}{|p \cdot q|} \qquad t_{CL} = \frac{E}{|p \cdot q|}, \tag{13}$$

Surprisingly, the Landau-Pomeranchuk formula is reproduced, see Eq. 6.

Among other approaches to give a quantitative evaluation of the FT one should mention the SKAT parameterization of the LAB frame FZ [53]:

$$l_{SKAT} = \frac{|\vec{p}|}{\mu^2}. \tag{14}$$

The value of the free parameter was found to be $\mu^2 = 0.08 \pm 0.04$ GeV^2 based on the experimental data for the multiplicity of low momentum (300 MeV/c $< p <$ 600 MeV/c) protons. This value of μ^2 agrees also with the analysis of the momentum distribution of negatively charged mesons in the region $p < 3$ GeV/c.

The SKAT formula can be translated to the following value of FT:

$$t_{SKAT} = \frac{E}{|\vec{p}|} l_{SKAT} = \frac{E}{\mu^2}, \qquad t_{SKAT,rest} = \frac{M}{\mu^2}. \tag{15}$$

Compared to the Rantf formula (Eq. 11) the SKAT parameterization corresponds to $p_T = 0$ but it also introduces a scale proportional to the hadron mass: $\tau_0 \leftrightarrow M/\mu^2$. According to the SKAT parameterization, FZ is identical for pions and nucleons with the same momentum. At $p \sim 1$ GeV/c FZ is expected to be ~ 2.5 fm, which is of the size of the carbon nucleus.

In another approach to model the FT, one postulates an effective (reduced) hadron-nucleon interaction cross section [54] at a distance z from the interaction point:

$$\sigma_{eff}(z) = \sigma_{free} \left(1 - \mathrm{e}^{-zMm_0/|\vec{p}|}\right) \tag{16}$$

with $m_0 \approx 0.4$ GeV.

Similar description of the FT (reduction of the cross section) is used in the quantum diffusion model [55]:

$$\sigma_{hN}^{eff}(z) = \sigma_{hN}$$

$$\times \left[\left(\frac{z}{l_h} + \frac{< n^2 k_t^2 >}{Q^2} (1 - \frac{z}{l_h}) \right) \theta(l_h - z) + \theta(z - l_h) \right], \tag{17}$$

where σ_{hN} is the free hadron-nucleon cross section, z is the distance from the interaction point, $k_t^2 \cong 0.35$ MeV/c is the average quark transverse momentum, $n = 2, 3$ for pions and nucleons. The value of the FT is determined by l_h which can be evaluated to be

$$l_h = 2p_h \left\langle \frac{1}{M_n^2 - M_h^2} \right\rangle, \tag{18}$$

where p_h and M_h denote hadron momentum and mass, and M_n is an intermediate state mass. The precise value of $\Delta M^2 = M_n^2 - M_h^2$ is not known and is estimated to be between 0.25 and 1.4 GeV^2. In [56] the values of 1 GeV^2 and 0.7 GeV^2 are used for protons and pions.

In the parameterizations given in Eqs (16) and (17) smaller effective cross section translates into a larger average distance to the first reinteraction point.

Recent experimental investigation of the effect in the semi-inclusive DIS scattering off nuclei was done in the HERMES experiment [57]. The measured quantity was the multiplicity ratio $R_M^h(\nu, Q^2, z, p_t^2)$ defined as:

$$R_M^h(\nu, Q^2, z, p_t^2) = \left(\frac{N_h}{N_e} \right)_A / \left(\frac{N_h}{N_e} \right)_D \tag{19}$$

with N_h and N_e the numbers of semi-inclusive hadrons at given (ν, Q^2, z, p_t^2) and of inclusive leptons at (ν, Q^2) for nuclear (atomic number A) and deuterium (D) targets. $z = E_h/\nu$ is a fraction of energy transfer carried by the hadron and p_t is the hadron momentum perpendicular to the momentum transfer. For pions, the data show a good agreement with the Lund model formula for the pre-hadron formation length:

$$L_c = z^{0.35}(1 - z)\frac{\nu}{\kappa} \tag{20}$$

with $\kappa \simeq 1.0 \frac{GeV}{fm}$.

In the case of pions produced via the Δ excitation and decay there is still another natural way to model the FT-like effect. In the INC picture one can treat Δ (like in the GiBUU approach [58]) as a real particle propagating some distance before it decays. The Δ lifetime in its rest frame is equal $\frac{1}{\Gamma}$, with $\Gamma \approx 120$ MeV, so in the LAB frame one obtains:

$$t_\Delta = \frac{E_\Delta}{M_\Delta \Gamma} \tag{21}$$

where E_Δ is the LAB frame Δ energy.

We conclude that various approaches lead to similar expressions for the FT as far as the dependence on hadron momentum is concerned but numerical coefficient and the size of the effect can be quite different.

B. FT models in MC event generators

Table III summarizes available information about FT models in major neutrino MC event generators.

MC	QE	RES[a]	DIS
NEUT	–	SKAT	SKAT
FLUKA	Coh length	Rantf	Rantf
GENIE	–	–	Rantf-like
NUANCE	1 fm	1 fm	1 fm

[a] Note that every MC has its own definition of what does the RES and DIS terms mean.

TABLE III. Formation Time models in various Monte Carlo event generators

NEUT uses the SKAT model both for RES and DIS [59].

FLUKA uses Eq. 13 for quasielastic scattering and Eq. 11 for other processes.

GENIE uses Eq. 11 but in a simplified form, neglecting p_T:

$$t_{\text{Genie}} = \tau_0. \tag{22}$$

GENIE assumes the value $\tau_0 = 0.342 fm/c$ [60]. One can check that for the pions the SKAT formula is reproduced. GENIE applies FZ to DIS events and also to the non-resonant background events in the RES dynamics [61].

NUANCE implemented an effective model in which the FZ is always equal to 1 fm [62].

C. NuWro FT model

In NuWro the formation zone effects are implemented:

- as coherence length (Eq. 13) for quasielastic scatterings
- as Δ propagation (Eq. 21) for RES interactions
- using Ranft model (Eq. 11) with a parameter τ for DIS

There is a smooth transition between the last two models at $W \simeq 1.6$ GeV.

With the Ranft model (without the approximation $p_T = 0$) the average value of FT depends both on neutrino energy and on hadron momentum. For a fixed value of the neutrino energy, lower hadron momenta correspond typically to larger values of the transverse momentum and smaller values of FT.

In order to fix the value of the parameter τ we analyze the NOMAD data for the backward moving pions.

Scenario	Without formation zone	With formation zone
1	37.2%	83.7%
2	43.3%	15.5%
2a	22.0%	8.1%
2b	15.6%	7.4%
2c	5.8%	0%
3	2.7%	0.7%
3a	1.9%	0.6%
3b	0.8%	0.1%
4	16.7%	0.1%

TABLE IV. Contribution to the sample of events with backward π^- from different scenarios (see the text)

1. *Comparison with NOMAD measurement of backward moving pions*

To fine tune our model of FZ we use the NOMAD experimental data [49]. The average neutrino energy is $\langle E_\nu \rangle = 24$ GeV and the target composition is dominated by carbon (64.30%) and oxygen (22.13%) with small additions of other elements.

We focus on the pion data. Our main observable is the average number of backward moving ($\cos\theta_{LAB} < 0$) negative pions Bπ^- with the momentum p_π between 350 and 800 MeV/c, as a function of Q^2. This observable is very sensitive to the FSI effects. Without FSI the number of backward moving pions would be small because they appear mainly due to nuclear reinteractions. Introduction of the FT makes the FSI effects smaller and reduces the number of Bπ^-.

Simulations made for various values of τ lead us to the conclusion that a good agreement with the data is obtained with $\tau \sim 8$ fm/c. Fig. 11 shows average numbers of backward moving π^- reported by NOMAD, and predicted by NuWro with and without FZ, as a function of Q^2. In order to better understand the NuWro performance various ways in which Bπ^- appear were analyzed:

1. pions are created in the primary vertex and undergo quasielastic scatterings
2. pions are created in FSI pion-nucleon interactions
   (a) single pion production
   (b) double pion production
   (c) triple pion production
3. pions are created in FSI nucleon-nucleon interactions
4. there are more FSI pion production processes.

Contributions from the above scenarios to events with backward moving π^- are listed in Table IV.

Table V shows the breakdown of the number of $B\pi^-$ in a single events. The NuWro predictions (with and without the FZ) are compared with the Nomad data [49].

$< \#B\pi >$	Data	NuWro	
		Without FT	With FT
0	939617	921048	937883
1	4238	22590	6126
2	164	375	8

TABLE V. Contribution to Bπ^- coming from events with 0, 1 or 2 pions

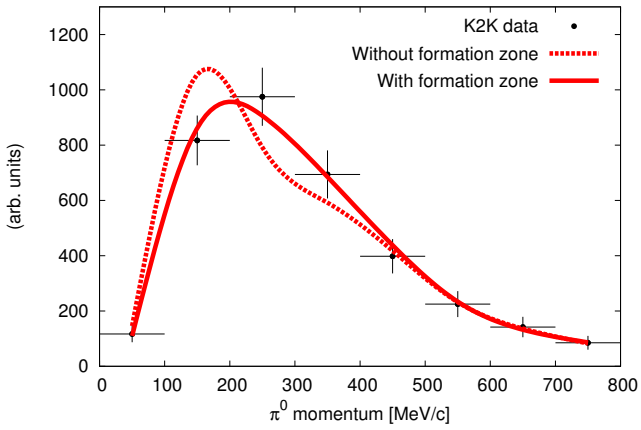

FIG. 14. (Color online) K2K: NC $1\pi^0$ production as a function of π^0 momentum; the data and NuWro predictions are normalized to the same area.

2. *Comparison with other MC event generators*

Figs 12 and 13 show the values of FZ in NuWro compared to other MC neutrino event generators. It is interesting that in the case of pions various models of FZ

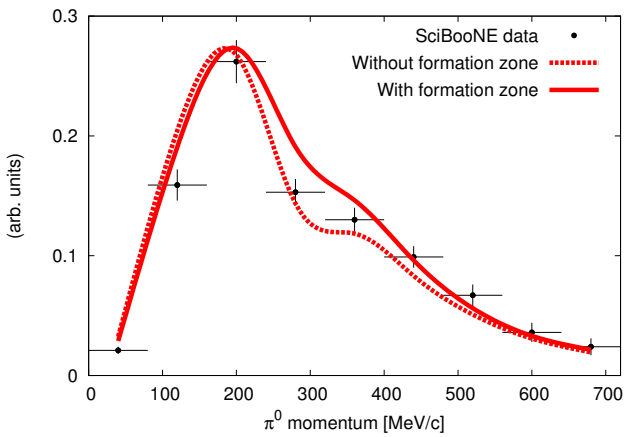

FIG. 15. (Color online) SciBooNE: NC π^0 production as a function π^0 momentum; the data and NuWro predictions are normalized to the same area.

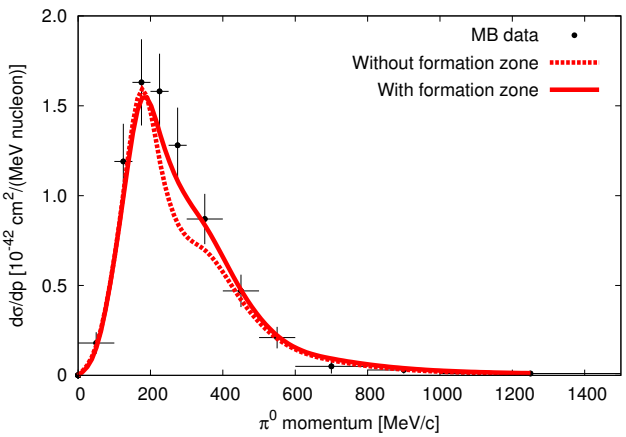

FIG. 16. (Color online) MiniBooNE (neutrino mode): NC $1\pi^0$ production as a function π^0 momentum.

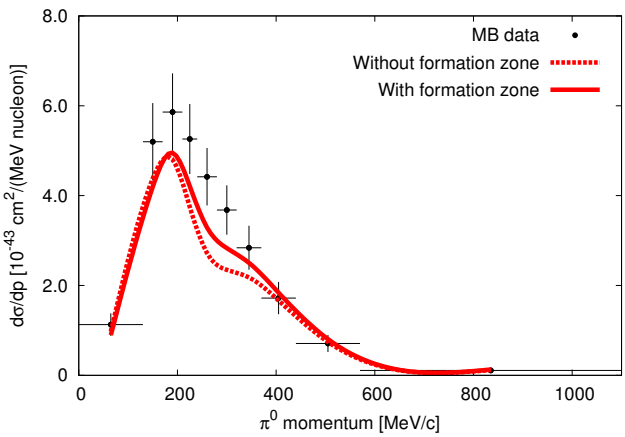

FIG. 17. (Color online) MiniBooNE (anti-neutrino mode): NC $1\pi^0$ production as a function π^0 momentum.

give very similar results, while in the case of nucleons the differences are much larger.

The NuWro results are given for a specific neutrino energy ($E_\nu = 1GeV$). The value of FZ grows with increasing E_ν due to the transverse momentum in the denominator, which goes to zero when hadron energy becomes higher.

In NuWro the dependence of the FZ on the pion kinetic energy is very flat.

V. APPLICATION: NC $1\pi^0$ PRODUCTION

A. Free nucleon NC π^0 production

The data for NC $1\pi^0$ production cross section on a free nucleon target is very scarce. The only such measurement was done in the Gargamelle bubble chamber. The target was in fact composed of C_3H_8 (90%) and CF_3Br but the FSI effects were subtracted [65].

In view of limitations in understanding of nuclear effects the results should be treated with caution. Notice that the data contain a contribution from the COH reaction. Originally, the results were presented as efficiency corrected relative production rates in several pion production channels [63]. The data re-analysis was done in [64]: information about neutrino flux was taken into account and the cross sections estimations were done.

Table VI shows the experimental data from [64] and NuWro predictions obtained for neutrinos of energy 2.2 GeV on free nucleon target and also on nucleons bound in ^{12}C, with Pauli blocking and Fermi motion effects taken into account, but without FSI effects. We find the agreement to be satisfactory. It is also possible to compare the NuWro predictions and the data for relative contributions from RES and DIS reaction channels. In the case of $\nu p \to \nu p \pi^0$ reaction the NuWro predictions for the RES:DIS ratio are: 78 : 22 for free and 82 : 18 for bound nucleons. The experimental data suggest $\sim 80 : 20$ (see Fig. 11 in [63]).

Channel	Cross section per nucleon ($\times 10^{-38} cm^2$)		
	Data	NuWro	
		free nucleon	bound nucleon
$\nu_\mu p \to \nu_\mu p \pi^0$	0.13 ± 0.02	0.15	0.12
$\nu_\mu n \to \nu_\mu n \pi^0$	0.08 ± 0.02	0.17	0.14
$\nu_\mu p \to \nu_\mu n \pi^+$	0.08 ± 0.02	0.13	0.11
$\nu_\mu n \to \nu_\mu p \pi^-$	0.11 ± 0.03	0.14	0.13
$\nu_\mu n \to \mu p \pi^0$	0.24 ± 0.04	0.38	0.36

TABLE VI. Single pion production cross sections. The data is taken from [64].

B. NC $1\pi^0$ production on a nucleus

Recent experimental data for the NC π^0 production come from three experiments. Basic information about them is summarized in Table VII.

Experiment	Beam	$\langle E_\nu \rangle$ [GeV]	Target	Normaliz.	Measurement
K2K [66]	ν_μ	1.30	H_2O	relative	dN/dT_π
MB [67]	ν_μ	0.81	CH_2	absolute	$d\sigma/dT_\pi$, $d\sigma/d\cos\theta_\pi$
MB [67]	$\bar{\nu}_\mu$	0.66	CH_2	absolute	$d\sigma/dT_\pi$ $d\sigma/d\cos\theta_\pi$
SciB [68]	ν_μ	0.81	C_8H_8	relative	dN/dT_π $dN/d\cos\theta_\pi$

TABLE VII. Recent NC π^0 production measurements.

In the K2K and MiniBooNE (MB) experiments the

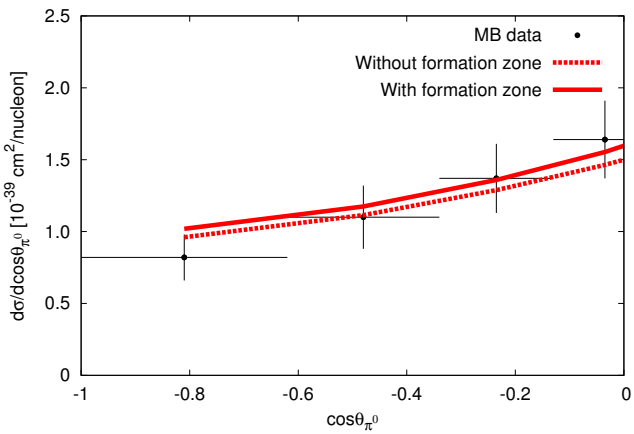

FIG. 18. (Color online) MiniBooNE (neutrino mode): NC $1\pi^0$ production as a function $\cos\theta$.

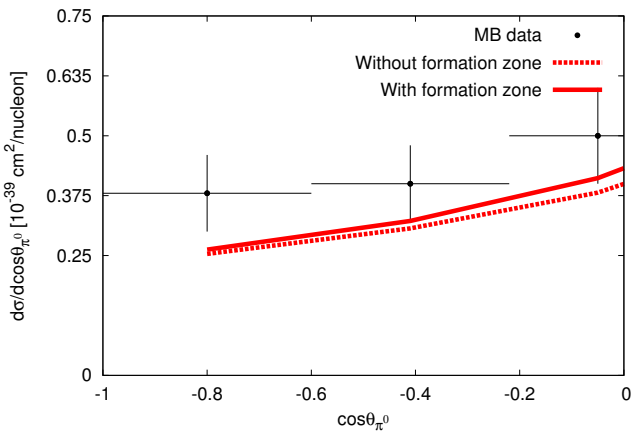

FIG. 19. (Color online) MiniBooNE (anti-neutrino mode): NC $1\pi^0$ production as a function $\cos\theta$.

signal was defined as exactly one π^0 leaving the nucleus target and no other mesons in the final state. In the case of SciBooNE (SciB) the signal was defined as *at least* one π^0 in the final state, with possible other pions as well.

The experimental signal for $1\pi^0$ production comes from: (i) single π^0 produced at the interaction point in the single pion production reaction; (ii) π^0 produced in double pion production reaction with other pion being absorbed; (iii) single $\pi^\pm$ production with charge exchange reaction $\pi^\pm \to \pi^0$ inside nucleus; (iv) primary quasi-elastic reaction with π^0 being produced due to nucleons re-interactions inside nucleus. For the $2\pi^0$ production the number of possible scenarios becomes larger.

According to NuWro, most of the $1\pi^0$ signal events $(93-95\%)$ come from the initial RES single pion production reactions, see Table VIII. In the case of the MB antineutrino flux the contribution is slightly smaller, because the antineutrinos are on average less energetic.

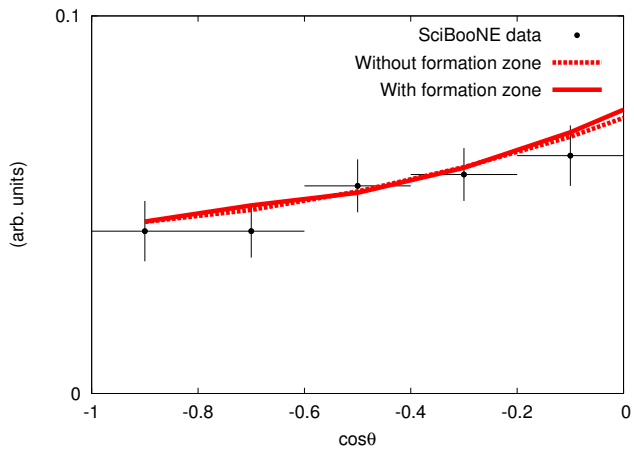

FIG. 20. (Color online) SciBooNE: NC π^0 production as a function $\cos\theta$.

Channel	K2K	MB ν	MB $\bar{\nu}$
$1\pi^0 \to 1\pi^0$	93.1% (84.5%)	93.0% (88.3%)	94.8% (92.4%)
no $\pi \to 1\pi^0$	2.0% (3.2%)	1.8% (2.4%)	1.2% (1.6%)
other $\pi \to 1\pi^0$	3.7% (6.8%)	4.2% (5.8%)	3.2% (3.9%)
more $\pi \to 1\pi^0$	1.2% (5.5%)	1.0% (3.5%)	0.7% (2.1%)

TABLE VIII. Origin of the signal events with $1\pi^0$ in the final state as predicted by NuWro. The values in brackets refer to results without FT.

Also, an impact of the FZ is in clear anti-correlation with the average projectile energy.

Table IX enumerates what can happen to a π^0 produced in the primary vertex due to the FSI effects. One can see that pion absorption (the second row) reduces the number of NC π^0 events, but the FZ makes the effect smaller. Also the charge exchange reaction (the third row) has a significant impact on the final states. It is clear that the NC π^0 production measurement provide a useful test for the FSI models.

Table X shows the breakdown of the NC π^0 signal in the SciB experiment as it is understood by NuWro. The second column contains the values reported by the SciB collaboration obtained from the MC they used in the data analysis (NEUT). Next two columns contain NuWro predictions both with and without FZ effects.

Channel	K2K	MB ν	MB $\bar{\nu}$
$1\pi^0 \to 1\pi^0$	81.6% (64.0%)	79.1% (66.9%)	83.0% (74.5%)
$1\pi^0 \to$ no π	5.9% (19.3%)	7.2% (19.2%)	6.4% (15.9%)
$1\pi^0 \to$ other π	10.1% (11.0%)	10.2% (10.1%)	9.6% (7.8%)
$1\pi^0 \to$ more π	2.4% (5.7%)	2.0% (3.7%)	1.0% (1.8%)

TABLE IX. An impact of FSI efects on the events with $1\pi^0$ in the primary interaction, as predicted by nuWro. The values in brackets refer to results without FT.

Channel	SciB MC	NuWro (no FT)	NuWro (FT)
$1\pi^0$	85%	80%	82%
$1\pi^0$ + charged π	11%	16%	14%
$2\pi^0$	4%	4%	4%

TABLE X. Breakdown of contributions to SciBooNE signal NC π^0 events as modeled by SciB and NuWro MCs.

NCπ^0/CC	K2K	SciB
Data	0.064±0.008	0.077 ± 0.010
NuWro (without FZ)	0.070	0.071
NuWro (with FZ)	0.079	0.077

TABLE XI. NCπ^0/CC cross section ratios reported by K2K and SciB and as predicted by NuWro.

K2K and SciBooNE did not publish the normalized differential cross section. Instead, flux averaged ratios of NCπ^0 to total CC cross sections were given. In the Table XI we compare both values with the NuWro results.

Figs 14–17 show the data and NuWro predictions for π^0 momentum distribution in various experiments.

In the case of the normalized cross section the main effect of the introduction of the FZ is the increase of the cross section in the pion absorption peak region. The effect can be estimated to be $10 - 15\%$. In the case of the K2K measurement the use of the FZ also moves the peak of the pion momentum distribution to larger values by about 50 MeV/c resulting in better agreement with the data.

Both MB and SciB experiments provide distributions of events versus the cosine of the angle between the neutrino and π^0 momenta. Figs 18–20 show pions angular distributions together with the NuWro predictions. We focus on the backward directions because we expected an important impact from FZ effects in this kinematical region.

Figs 18 and 19 show that the FZ increases the NC π^0 production in the backward directions but the effect is rather small. The reason is that at lower neutrino energies there are many backward moving π^0 even without FSI effects. We checked that only for larger Q^2 values the FSI become the main *source* of π^0 and FZ reduces their number.

In Fig. 20 the NuWro results are normalized to the number π^0 predicted to be in the data. In this case using the FZ makes the absolute number of backward moving π^0's little larger, but the effect can hardly be seen.

VI. CONCLUSIONS

Any comparison to recent NC π^0 production data requires a computational tool capable of modeling several dynamical mechanisms for neutrino-nucleon interaction as well as the FSI effects. The NuWro MC event generator has all the required physical models implemented and it was demonstrated that it reproduces the experimental results quite well. An important ingredient of the NuWro FSI model is the FZ mechanism which even at relatively small neutrino energies typical for K2K, MB and SciB experiments leads to sizable effects on the π^0 in the final state. We hope that our results will be useful for better evaluation of the systematic error coming from the NC π^0 production in neutrino oscillation experiments like T2K.

ACKNOWLEDGMENTS

The authors were partially supported by the grants: N N202 368439 and 2011/01/M/ST2/02578.

[1] H. Gallagher, AIP Conf. Proc. **1189** (2009) 35.
[2] A.M. Ankowski, PoS(NUFACT08) 118 (2008).
[3] P. de Perio, AIP Conf. Proc. **1405** (2011) 223.
[4] A. Ferrari, P.R. Sala, A Fasso', and J. Ranft, CERN-2005-010, INFN/TC_05/11 (2005); G. Battistoni, P.R. Sala, M. Lantz, and G. Smirnov, Acta Phys. Pol. B**40** (2009) 2491.
[5] D. Casper, Nucl. Phys. B (Proc. Suppl.) **112** (2002) 161; P. Przewłocki, Acta Phys. Pol. B**40** (2009) 2513.
[6] Y. Hayato, Nucl. Phys. B (Proc. Suppl.) **112** (2002) 171; Acta Phys. Pol. B **40** (2009) 2477.
[7] C. Andreopoulos et al., Nucl. Instrum. Meth. A**614** (2010) 87.
[8] N. Metropolis et al., Phys. Rev. **110** (1958) 185 and 204;
[9] R.J. Glauber, in Lectures in Theoretical Physics, Vol. I, edited by W.E. Brittin and L.G. Dunham (Interscience, New York, 1959), p. 315.
[10] L.L. Salcedo, E. Oset, M.J. Vicente-Vacas, and C. Garcia-Recio, Nucl. Phys. A**484** (1988) 557
[11] A.H. Mueller, in Proceedings of the Seventeenth Recontre de Moriond Conference on Elementary Particle Physics, Les Arcs, France, 1982 edited by J. Tran Thanh Van (Editions Fronriers, Gif-sur-Yvette, France, 1982); S. J. Brodsky, in Proceedings of the Thirteenth International Symposium on Multiparticle Dynamics, Volen- dam, The Netherlands, 1982, edited by W. Kittel et al. (World Scientific, Singapore, 1983).
[12] X.Qian, et al, Phys.Rev. C**81** (2010) 055209.
[13] L. Stodolsky, *Formation Zone Description in Multiproduction*, Talk at the VIIth International Colloquium on Multiparticle Reactions, Oxford, July 1975
[14] J. Ranft, Z. Phys. C**43** (1989) 439.
[15] V.V. Lyubushkin [NOMAD collaboration] Eur.Phys.J. C**63** (2009) 355.
[16] J.D. Zumbro et al, Phys. Rev. Lett **71** (1993) 1796; Bao-An Li, W. Bauer, and Che Ming Koa, Phys. Lett. B**382** (1996) 337; S.G. Mashnik, R.J. Peterson, A.J. Sierk, and M.J. Braunstein, Phys. Rev. C**61** (2000) 034601.

[17] C. Juszczak, J.A. Nowak, and J.T. Sobczyk, Nucl. Phys. B (Proc. Suppl.) **159** (2006) 211; J.A. Nowak, Phys. Scr. T**127** (2006) 70; C. Juszczak, Acta Phys. Pol. B**40** (2009) 2507;

[18] O. Benhar, A. Fabrocini, S. Fantoni, and I. Sick, Nucl. Phys. A **579** (1994) 493; D. Rohe et al. (E97-006 Collaboration), Phys. Rev. Lett. **93** (2004) 182501; D. Rohe, for the E97-006 Collaboration, Nucl. Phys. B (Proc. Suppl.) **159** (2006) 152.

[19] C. Juszczak, J, Nowak, and J.T. Sobczyk, Eur. J. Phys. C**39** (2005) 195.

[20] http://gwdac.phys.gwu.edu/

[21] S.J. Barish et al., Phys.Rev.D 19 (1979) 2521

[22] S.J. Barish et al., Phys.Rev.D 16 (1977) 3103

[23] N.J.Baker et al. Phys.Rev.D 25 (1982) 617

[24] NOMAD Collaboration: Q.K. Wu et al, Phys.Lett.B 660 (2008) 19-25

[25] SciBooNE Collaboration: Y. Nakajima et al, Phys.Rev.D 83 (2011) 012005

[26] MINOS Collaboration: P. Adamson et al, Phys.Rev.D 81 (2010) 072002

[27] C.H. Llewellyn Smith, Phys. Rep. **3** (1972) 261.

[28] H. Budd, A. Bodek, and J. Arrington, *Modeling Quasi-elastic Form Factors for Electron and Neutrino Scattering*, hep-ex/0308005.

[29] R. Bradford, A. Bodek, H.S. Budd, and J. Arrington, Nucl. Phys. Proc. Suppl. **159** (2006) 127.

[30] W.M. Alberico, S.M. Bilenky, C. Giunti, and K.M. Graczyk, Phys. Rev. C**79** (2009) 065204.

[31] A.M. Ankowski and J.T. Sobczyk, Phys. Rev. C**77** (2008) 044311.

[32] T. de Forest, Jr., Nucl. Phys. A**392** (1983) 232.

[33] K.M. Graczyk, D. Kiełczewska, P. Przewłocki, and J.T. Sobczyk, Phys. Rev. D**80** (2009) 093001.

[34] D. Rein and L.M. Sehgal, Annals of Physics **133** (1981) 79.

[35] K.M. Graczyk, C. Juszczak, and J.T. Sobczyk, Nucl. Phys. A**781** (2007) 227.

[36] A. Bodek, U.K. Yang, Nucl. Phys. B Proc.(Suppl) **112** (2002) 70.

[37] F. Sartogo, *Interazioni di neutrini atmosferici: un modello fenomenologico e la sua applicazione nell'interpretazione dei dati ottenibili in rivelatori sotterranei* (in Italian), PhD Thesis, supervisor P. Lipari, Rome.

[38] J.A. Nowak, Phys. Scr. T**127** (2006) 70 J.T. Sobczyk, PoS(NUFACT08) 141 (2008).

[39] D. Rein and L.M. Sehgal, Nucl. Phys. B**223** (1983) 29.

[40] E. Oset, L.L. Salcedo, D. Strottman, Phys. Lett. B**165** (1985) 13; E. Oset, L.L. Salcedo, Nucl. Phys. A**468** (1987) 631.

[41] D. Ashery et al, Phys. Rev. C**23** (1981) 2173; D. Ashery et al, Phys. Rev. C**30** (1984) 946.

[42] I. Navon, et al, Phys. Rev. C**28** (1983) 2548.

[43] M.K. Jones et al, Phys. Rev. C**48** (1993) 2800.

[44] R.A. Giannelli, et al, Phys. Rev. C**61** (2000) 054615.

[45] S.M. Levenson, et al, Phys. Rev. C**28** (1983) 326.

[46] M. Ikeda, *Measurement of π-N interactions: PIAν0-Harpsichord*, a talk given at NuFact11, XIIIth Workshop on Neutrino Factories, Superbeams and Beta-beams, 1-6 August 2011, Geneva.

[47] L. Landau and I. Pomeranchuk, Doklady Akademii Nauk SSR **92** (1953) 535; ibid **92** (1953) 735.

[48] A. Fasso et al, *The physics models of FLUKA: status and recent developments*, arXiv hep-ph/0306267.

[49] P. Astier et al., [NOMAD Collaboration], Nucl. Phys. B**609** (2001) 255.

[50] A. Bialas, Z. Phys. C**26** (1984) 301.

[51] G. Battistoni, P.R. Sala, and A. Ferrari, Acta Phys. Pol. B**37** (2006) 2361.

[52] G. Battistoni, A. Ferrari, A. Rubbia, and P.R. Sala, *The FLUKA nuclear cascade model applied to neutrino interactions*, talk given at NuInt02, http://www.ps.uci.edu/ nuint/proceedings/sala.pdf

[53] D. S. Baranov, et al, *An Estimate For The Formation Length Of Hadrons In Neutrino Interactions*, PHE 84-04, 1984.

[54] A. El-Naghy and S.M. Eliseev, J. Phys. G: Nucl. Part. Phys. **16** (1990) 39.

[55] G. R. Farrar, H. Liu, L.L. Frankfurt, and M.I. Strikman, Phys. Rev. Lett. **61** (1988) 686.

[56] W. Cosyn, M C. Martinez, J. Ryckebusch, and B. Van Overmeire, Phys. Rev. C**74** (2006) 062201.

[57] A. Airapetian et al [HERMES collaboration], Nucl. Phys. B**780** (2007) 1.

[58] O. Buss et al, *Transport-theoretical Description of Nuclear Reactions*, to appear in Physics Reports, arXiv:1106.1344 [hep-ph].

[59] Y. Hayato-san, private communication.

[60] C. Andreopoulos et al, Nucl. Instrum. Meth. A**614** (2010) 87;

[61] C. Andreopoulos, private communication.

[62] G. Zeller, private communication.

[63] W. Krenz et al, Nucl. Phys. B**135** (1978) 45.

[64] E.A. Hawker, *Single Pion Production in Low Energy ν Carbon Interactions*, talk given at NuInt02, http://www.ps.uci.edu/ nuint/proceedings/hawker.pdf. See also W. Lerche et al., Phys. Lett. B**78** (1978) 510.

[65] S.L. Adler, S. Nussinov, and E.A. Paschos, Phys. Rev. D**9** (1974) 2125.

[66] S. Nakayama et al. [K2K collaboration], Phys. Lett. B**619** 255.

[67] A.A. Aguilar-Arevalo et al [MiniBooNE collaboration], Phys. Rev. D**81** (2010) 013005.

[68] Y. Kurimoto, et al [SciBooNE collaboration], Phys. Rev. D**81** (2009) 033004.